

# Numerical Simulation of the Wake of Non Equipotential Spacecrafts in the Ionosphere

A. Soubeyran, L. Lévy

*Département d'Etudes et de Recherches en Technologie Spatiale, Centre d'Etudes et de Recherches de Toulouse, 2 av. E. Belin, 31055 Toulouse Cedex, France*

E. Coggiola

*# 245, Petrie Science Building/ Physics Department/ North York, Ontario/M3J 1P3/ Canada*

## ABSTRACT

We studied the spacecraft/plasma interaction in the particular case of differential charging of satellites in Low Earth Orbit. The environment of such a satellite is very anisotropic, especially because of the mesosonic character of his velocity. We have tried to investigate numerically this "worst case" situation for infinite cylinders and spheres.

The code which we have developed, solves selfconsistently the coupled Hamilton and Poisson equations, in polar coordinates. It takes into account a differential polarisation on the rearward side of the spacecraft, where it is most likely to appear. Electrons are supposed in thermal equilibrium.

It follows from our simulations performed with this code, that the wake of a satellite in L.E.O. is generally shorter than expected from simple thermal considerations. For middle class satellites, severe disturbances could occur, which remain confined in the ionic shadow of the spacecraft. The wake density is decreasing when the differential potential is increasing. For a small mock-up, the potential disturbances could extend well out of the wake. The wake density increases with the backward side polarisation.

The near wake is always empty of drifting ions, so it seems likely that the back side charge cannot be neutralized by such ions.

## 1. INTRODUCTION

Owing a large number of failures on geostationaries spacecrafts, the interactions between them and the plasma at these altitudes were largely studied and today mainly understood as result of energetic electrons precipitations (see for example Fennel et al. 1983, and Levy et al. 1986). A first analysis of such interactions at ionospheric altitudes leads to the conclusion that, except perhaps in very special conditions (as for DMSP, Gussenhoven et al. 1985, and Yeh et al. 1987), the absolute potential of an equipotential satellite must remain around a few negative volts. This is due to the smallness of the Debye length with respect to the spacecraft dimensions, in this colder and denser plasma (Al'Pert et al. 1965) (table 1). Despite these reassuring conclusion, and the fact that no failures due to anomalous charging was actually reported on low earth orbit (L.E.O.), we decided to investigate the case of non equipotential spacecrafts (already tackled by L.W. Parker 1978, 1983). Contrary to the geostationary case, the plasma environment of a spacecraft in the ionosphere, is very anisotropic : due to the mesosonic character of the spacecraft speed, a wake appears behind it, where the conditions could approach those of the geostationary plasma (Samir et al. 1986). In such a rarefacted medium, high charging levels are likely to occur, especially during auroral precipitation of energetic electrons, on insulated parts (floating metalizations or dielectrics) (Coggiola 1988) (figure 1). On futur spacecrafts, active polarisation may also induce high voltages on parts of the external surface.

To better understand the interaction between the wake and such polarisations, and therefrom deduce whether ambient ions could be dragged to such charged area on the wake side or not, we developed a suitable numerical simulation.

## 2. NUMERICAL MODEL

In low orbit conditions, the space-charge coupling, the magnetic field effects, and the ion flow effects could all be important. As a result, modelling of spacecraft-environment interactions appears likely to be a difficult task (Laframboise 1983). Therefore, we must use some approximations to develop our numerical simulation.

### 2.1. Simplifications

- 1- The spacecraft is equipotential, with a main surface at the rear of the spacecraft, at various fixed negative potentials, up to -1kV.
- 2- We assume no magnetic field and
- 3- no secondary emission or photo-emission of electrons.
- 4- In such conditions, we choose spherical or infinite cylindrical structures to obtain a purely bidimensional geometry, which reduces greatly the computation work.
- 5- Moreover, we decided to limit the computation area to the back side of the spacecraft, around the wake. So, all effects arising in front of the spacecraft are neglected. This seems to be realistic because of the thinness of the sheath on this side.
- 6- We assume only one sort of ions ( $O^+$  or  $Ar^+$ ) with a drift velocity and eventually a small thermal component.
- 7- The electrons are supposed in thermal equilibrium, and so modeled using the Boltzmann factor.
- 8- The plasma is collisionless on the scale of the interaction area.

The modeled situation could be considered as a "worst case" for the differential charging of a non equipotential satellite. The charge is located in the ion depleted wake, where it is likely to appear under auroral precipitation (Katz et al. 1985), and it could only be limited by collection of drifting ions of the ambient plasma.

Under these assumptions, we developed the following numerical algorithm.

### 2.2. Algorithm Description

This code solves selfconsistently the coupled Hamilton and Poisson equations, in polar coordinates.

As seen above, the simplified geometry of the interaction is bidimensional (2d2v) and, as we have already a physical discontinuity of the voltage on the spacecraft surface, we choose to solve the equations in polar coordinates, to avoid a second, geometrical, discontinuity. These coordinates result either from cylindrical coordinates invariant along Z, or from spherical coordinates invariant around the system axis as shown on figure 2.

In the collisionless medium which is being treated, the particles density and velocity distributions are well described by the kinetic theory, expressed through the Vlasov equation (Delcroix 1963). But this form is difficult to solve directly for a complex system, and we replace it by the integration of Hamilton's motion equations over a large number of simulation particles. These particles (equivalent to real ions packets) are all introduced during one first time step. They form a charging front which is moved over the computational mesh by integrating the Hamilton's equations, taking into account the fixed electric fields deduced from a potential distribution.

At each time step, each particle leaves a charge on the four nearest grid points by means of a bilinear deposition scheme (PIC method described by Birdsall and Langdon

1985, see fig). When all particules of the front have reached the boundaries (satellite surface or external boundary), we sum at each grid point the charges accumulated during the process on all trajectories. After some weighing by the cell surfaces and normalisation, the ionic density is deduced at all nodes.

This is used as input for the Poisson equation which is expressed in a finite-difference form over the same grid as above. Owing to the Boltzmann factor (electronic density), the resulting system of equations is not linear. Nevertheless, it can be solved by a Gauss-Seidel algorithm. We thus obtain a discrete potential distribution which gives us the electric field at any place in the computation area, through a finite differentiation, and eventually a bilinear interpolation if the point is not at a node. This is used in its turn, as input for the integration of Hamilton equations.

For the first iteration of this algorithm (figure 3), we choose everywhere a zero potential, and so a zero electric field. Then we perform the above scheme until self-consistence is achieved : the density distribution must give, using the Poisson equation, a potential distribution which gives back, after the integration of Hamilton equations, the same density distribution.

In relation with the assumptions made before, with computational capacities, and with observations of preliminary results, we are able to set rough estimations of limits to the input parameters.

### 2.3. Limits of the Simulation

As seen from the boundary conditions, there is no treatment of the forward region of the spacecraft, and we assume a cylindrical (resp. plane) symmetry around the drift direction, behind a sphere (resp. an infinite cylinder). These remarks lead to the quarter shaped working area of figure 2.

All the boundary conditions are independent of time and so we obtain only stationary results. These could eventually be approximations in particular cases.

All the calculations are made with dimensionless normalized variables and parameters, in order to simplify the formulation, and make comparisons easier. The interaction parameters are limited as it follows :

$$100 \geq \zeta = R_{\text{sat}} / L_{\text{Debye}} \geq 10$$

The upper bound is due to limits in computational capacities, because the spatial grid step must be taken of the order of the Debye length :  $L_D$  (Birdsall and Langdon 1985). The lower bound comes from physical considerations about the thickness of the sheath (a few  $L_D$ ), and his effects in front of the spacecraft which we neglect (Al'Pert et al. 1965).

$$40 \geq M_i = V_{\text{sat}} / V_{\text{th},i} \geq 5$$

As above, the upper bound comes from computational limitation, because the interesting area may reach about  $(M_i R_{\text{sat}})$  behind the spacecraft (Gurevich et al. 1969, and Samir et al. 1981). The lower bound was deduced from tests which showed that for low values of  $M_i$ , particules seem to be trapped near the axis of the wake, and prevent the algorithm from converging. This can result from turbulences and/or inadequate space sampling and to few particules.

$$5 \geq \eta_c = -e\phi_{\text{conduct}} / kT \geq 0$$

The upper bound is necessary for the thickness of the plasma sheath to remain of the order of the Debye length. The lower bound is dictated by the assumption of a thermal equilibrium for the electrons.

$$1000 \geq \eta_d = -e\phi_{\text{diel}} / kT \geq 0$$

The upper bound was deduced again from observations of trapped particules at "focal point-like features" on the axis of the wake, which we suspect to give rise to

some turbulence phenomena. The lower bound comes as above from the approximation of the electronic density by the Boltzmann factor.

All these constraints are broad approximations, subject to evolutions in relation with improvements of the code.

We will now examine a few interesting results of our code. These are only early calculations, and they will need further investigations.

### 3. RESULTS AND DISCUSSION

We present here two configurations, corresponding to two very different situations, showing the versatility of our code. The first one is corresponding to a middle-class satellite in the ionosphere, the second one could be interpreted as a mock-up in the plasma stream of an experimental chamber.

#### 3.1. Middle-Class Satellite in the Ionosphere (see table 2 and figures 4 a-f)

The three backside potentials have been chosen to represent :

- equipotential structure at floating potential
- active polarisation coming from experiments or power supply
- charging under energetic electrons precipitation

The main surface is fixed at the floating potential, and this seems to influence the wake shape as already pointed out by Stone (1981). Indeed, we observe a wake void shorter than would be expected from simple thermal calculations (i.e.  $Mi.R_{sat}$ ), even for an equipotential satellite (fig. 4 b). This length is better obtained by taking into account the floating potential and the negative space charge of the wake :

$$L_{wake} = \frac{V_{//}}{V_{\perp}} = \sqrt{\frac{E_{drift}}{E_{float.} + E_{wake}}} = \sqrt{\frac{5.3}{.36 + .6}} = 2.3$$

and we observe :  $L_w \approx 2.5$  in good agreement with the calculated length.

Between  $L_w$  and  $Mi.R_{sat}$  (limits of our system), we observe a very inhomogeneous wake, with a strong focusation on the axis, behind the sphere. In the case of a cylinder, the geometry leads to a lower axial concentration, but the potential disturbance is more extended and it results in lower densities around the axis, but the wake is wider.

When the differential polarisation grows up, the potential disturbance extends but remains mainly confined in the ionic "shadow" of the spacecraft (fig. 4 c,e). So, the flux of particules which enters the wake doesn't increase very much, but these particules are more and more accelerated. Thus, their local density decreases around the central axis, where they tend to accumulate in localized areas (fig. 4 d,f). Perhaps is it an indication of axial turbulence ? Indeed, for very high potentials (-1kV) the density distribution given by the code is not really stable. Nevertheless, it seems that the polarised surface remains always in a near wake almost empty of ions and is not expected to be discharged through a current coming from the drifting ions.

#### 3.2. Mock-up in a Stream of Drifting Ions in a Plasma Chamber (see table 3 and figures 5 a-f and 6 a-d)

In this case, the main surface remains at zero potential, and we fixed for the rearward surface the same potentials as before. We find this time that for a structure wholly at zero potential, the shape of the near wake is controled both by the backward negative space charge and by the thermal motions :

$$L_w \approx \sqrt{\frac{E_{\text{drift}}}{E_{\text{th.i.}} + E_w}} \approx \sqrt{\frac{42}{.1 + .3}} = 10.$$

and we observe :  $L_w \approx 9$  (fig. 5 b, 6 b)

When the differential potential is growing up, the particles are driven toward the wake axis with increasing velocities, as above for a satellite. But now, the mock-up is too small ( $\zeta_{\text{mock-up}} < \zeta_{\text{spacecraft}}$ ) to shield the potential disturbance for high potentials, and this extends well out of the wake (fig. 5 e) and even around the mock-up itself for a cylindrical geometry (fig. 6 c). So, the flux of ions entering the properly so called wake, increase simultaneously with their speed, and the ionic density is not decreasing as above, but on the contrary, generally increasing too (fig. 5 f), except for very high polarised cylinders (fig. 6 d).

For both studies, a differential polarisation limited to a few tens of volts does not affect the wake; some modifications begin to appear around hundred volts (fig. 4 c,d and 5 c,d).

We never observed any collection of ions on the polarised rearward surface, which is always remaining in a near-wake empty of particles, limited by our sensitivity : i.e.  $(.03 \cdot N_0)$  around the spacecraft and  $(.003 \cdot N_0)$  around the mock-up. This seems to be due to the fact that ions which experience the potential disturbance are accelerated at first almost along the drift direction and slightly repelled from the spacecraft surface, because of the shape of the isopotentials around the satellite. After this acceleration, the potential crossed by the particles is decreasing and not strong enough to attract them back. Moreover, the potential decreases very rapidly near the polarised surface and the ions do only cross regions of potential lower than their own drifting energy. For higher potentials, or different geometries, this result could become invalide.

#### 4. CONCLUSIONS

In the limits expressed before (§2.3.), the code which we developed gives interesting new results about the wake structure of a non equipotential probe in a drifting plasma. We conclude that :

- 1- For a differential potential lower than 100 Volts, the wake disturbance remains weak.
- 2- For higher potentials, the disturbance depends mainly on the  $\zeta = R_{\text{sat}}/L_{\text{Debye}}$  parameter :
  - For low  $\zeta$  ( $\leq 10$ ) the potential disturbance extends in the plasma around the wake, and the density in the wake increases with the differential potential.
  - For high  $\zeta$  ( $> 10$ ) the probe shields the potential disturbance which remains confined in the near-wake, and the density in the mid-wake decreases when the potential increases.

However, the density is always increasing with the potential on the axis behind a sphere, because of focusing effects. Furthermore, these conclusions concern mainly the spherical probe. It seems probable that the transition value of  $\zeta$  is higher for a cylinder, due to the fact that, at equal applied potential, the disturbance is far more extended around a cylinder than around a sphere. In this case, there is a competition between lower geometrical condensation, but higher electric field focusing effect.

3- Last but not least, even for differential potentials as high as -1kV, we do not observe any discharging current coming from the drifting ions. This confirms the possibility of high differential potentials on spacecrafts, in particularly hard conditions, such as shadow and energetic electrons precipitations without enough secondary emission. It is although obvious that any ionic population without drift

movement with respect to the probe ( plasma emitted from it or resulting from ionisation or charge exchange on non drifting neutrals...) will probably be very sensitive to the potential hole in the wake and could strongly modify the above results as suggested by the results of experiments of Coggiola (1988).

#### REFERENCES

- Al'Pert, Y.A., Gurevich, A.V., and Pitaevskii, L.P., "Space Physics with Artificial Satellite", Consultant Bureau, New York, 1965.
- Birdsall, C.K., and Langdon, A.B., "Plasma Physics via Computer Simulation", McGraw-Hill, New York, 1985.
- Coggiola, E., "Etude Théorique et Expérimentale de l'Écoulement de Plasma autour d'un Cylindre Non Equipotentiel", Thèse doctorat ENSAE, CERToulouse/DERTS, 16 Juin 1988.
- Delcroix, J.L., "Physique des plasmas I", Monographie Dunod, Paris, 1963.
- Fennel, J.F., Koons, H.C., Leung, M.S., and Mizera, P.F., "The Aerospace Corporation - A Review of SCATHA Satellite results : Charging and Discharging", ESA-SP-198, Noordwijk, The Netherlands, Sept. 1983.
- Gurevich, A.V., Pitaevskii, L.P., and Smirnova, V.V., "Ionospheric Aerodynamics", Space Sci. Rev., Vol. 9, P. 805, 1969.
- Gussenhoven, M.S., Hardy, D.A., Rich, F., Burke, W.J., and Yeh, H.-C., "High-Level Spacecraft Charging in the Low-Altitude Polar Auroral Environment", J. Geophys. Res., Vol. 90, N° A11, P. 11009, 1985.
- Katz, I., Mandell, M.J., Jongeward, G.A., and Lilley, Jr., J.R., "Astronaut Charging in the Wake of a Polar Orbiting Shuttle", AIAA-85-7035-CP, S-CUBED, AIAA Shuttle Environment And Operations II Meeting, Nov. 13-15, 1985.
- Laframboise, J.G., "Is There a Good Way to Model Spacecraft Charging in the Presence of Space-Charge Coupling, Flow, and Magnetic Fields", Proc. Air Force Geophys. Lab., Report N° AFGL-TR-83-0046, P. 57, 1983. ADA134894
- Levy, L., Sarraill, D., Philippon, J.P., Catani, J.P., and Fourquet, J.M., "Sur la Possibilité de Charge Différentielle de Plusieurs Kilovolts dans le Secteur Jour de l'Orbite Géosynchrone", AGARD Conference on "The Aerospace Environment at High Altitudes and its Implications for Spacecraft Charging and Communication", The Hague, The Netherlands, P. 17-1/12, 2-6 June 1986.
- Parker, L.W., "Differential Charging and Sheath Asymetry of Non-Conducting Spacecraft Due to Plasma Flows", J. Geophys. Res., Vol. 83, N° A10, P. 4873, 1978.
- Parker, L.W., "Contributions to sheath and Wake Modelling", Eur. Space Agency Spec. Publ., ESA SP-198, P. 81, 1983.
- Samir, U., Wildman, P.J., Rich, F., Brinton, H.C., and Sagalyn, R.C., "About the Parametric Interplay Between Ionic Mach Number, Body Size, and Satellite

- Potential in Determining the Ion Depletion in the Wake of the S3-2 Satellite", J. Geophys. Res., Vol. 86, N° A13, P. 11161, 1981.
- Samir,U., Stone,N.H., and Wright,Jr.,K.H., "On Plasma Disturbances Caused by the Motion of the Space Shuttle and Small Satellites : A Comparison of In Situ Observations", J. Geophys. Res.,Vol. 91, N° A1, P. 277, Jan. 1, 1986.
- Stone,N. H., "The Plasma Wake of Mesosonic Conducting Bodies, Part 1, An Experimental Parametric Study of Ion Focusing by the Plasma Sheath", J. Plasma Phys., Vol. 25, P. 351, 1981.
- Yeh,H.C., and Gussenhoven,S.M., "The Statistical Environment for Defense Meteorological Satellite Program Eclipse Charging", J. Geophys. Res., Vol. 92, N° A7, P. 7705, 1987.

**FIGURE 1 :**

Ion flow effects in low earth polar orbit

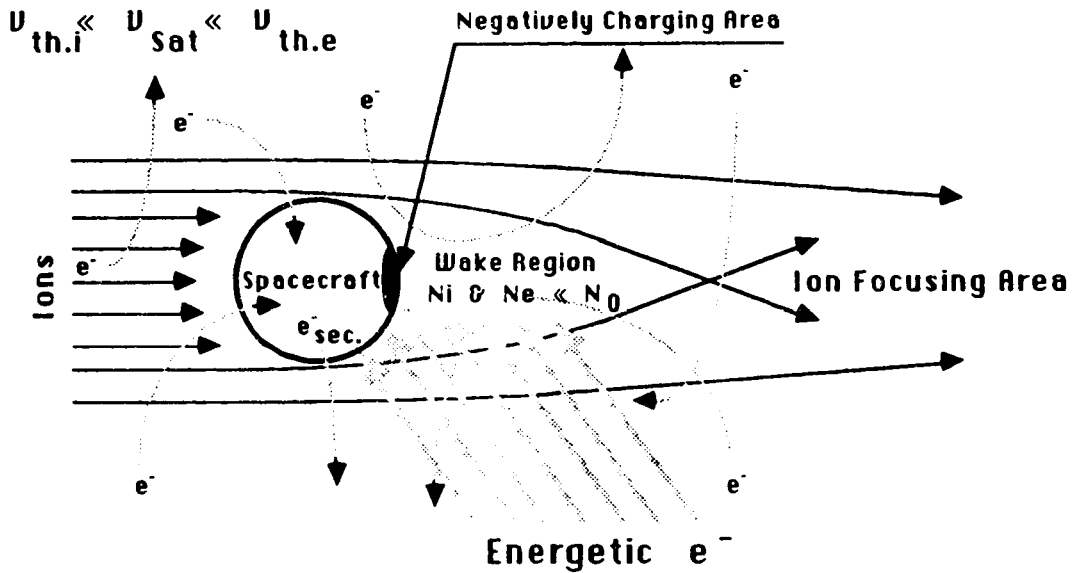


**FIGURE 2 :**

Diagram of the calculation area. It shows the polar computational mesh and the boundary conditions. The entrance frontier for particles (ions) is tint.

$R_{sat}$  : spacecraft radius

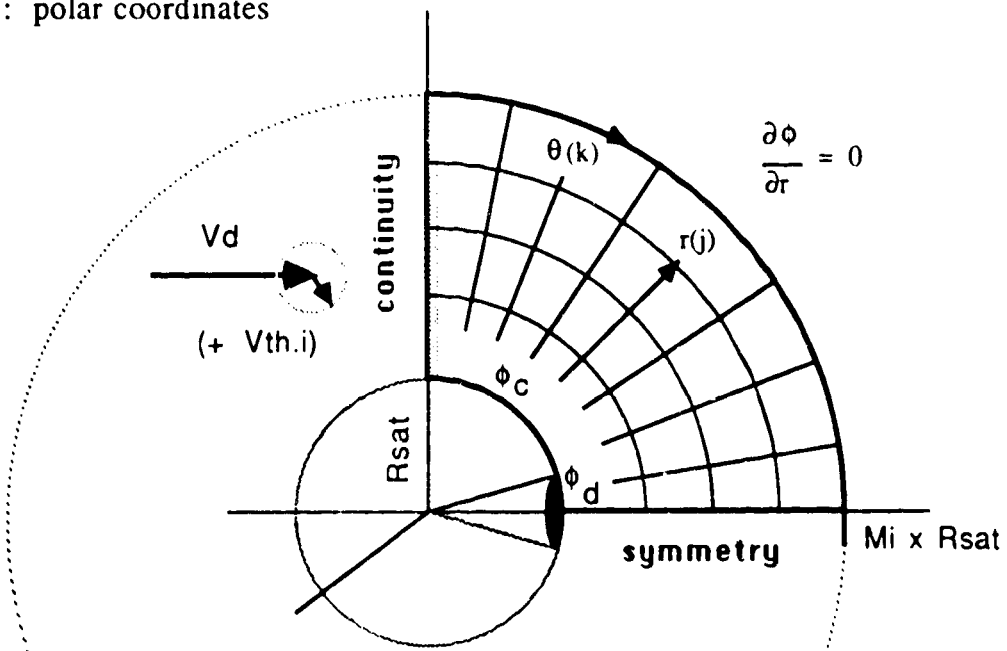
$V_d = -V_{sat}$  : ion drift velocity

$V_{th.i}$  : ion thermal velocity

$M_i = V_{sat} / V_{th.i}$  : ionic MACH number

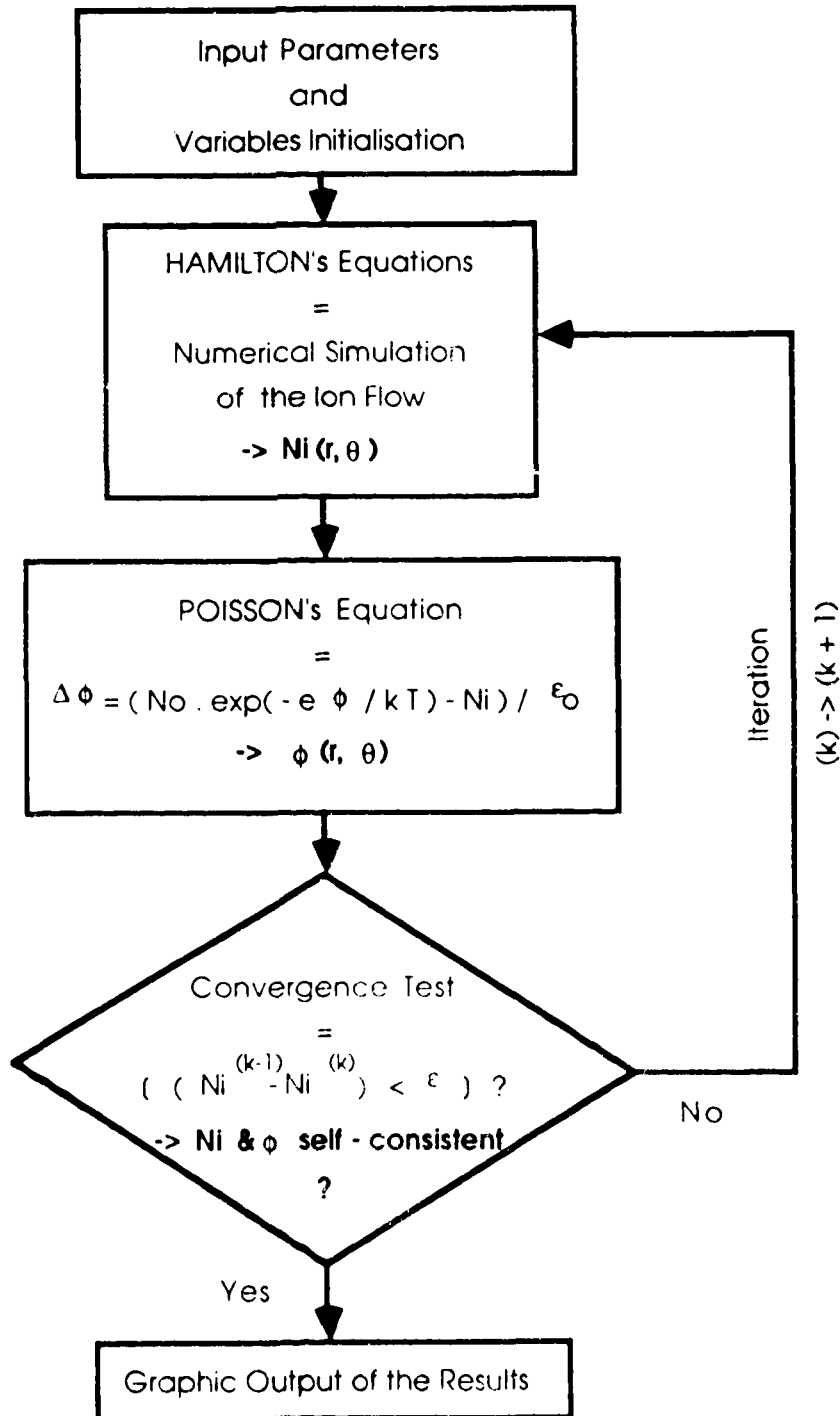
$\phi_c$  &  $\phi_d$  : potentials of the main structure and of the isolated part

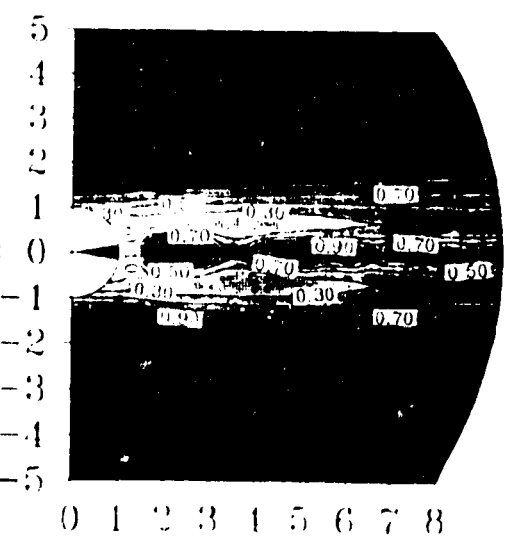
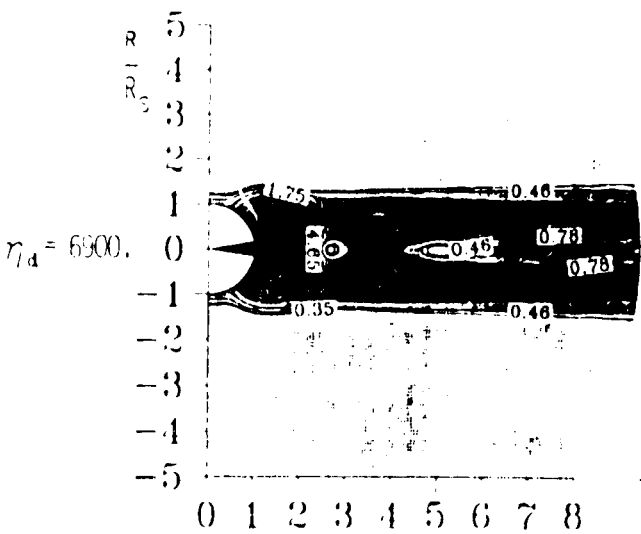
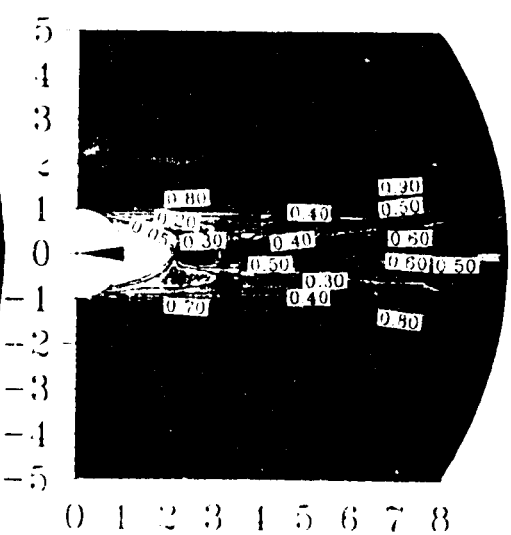
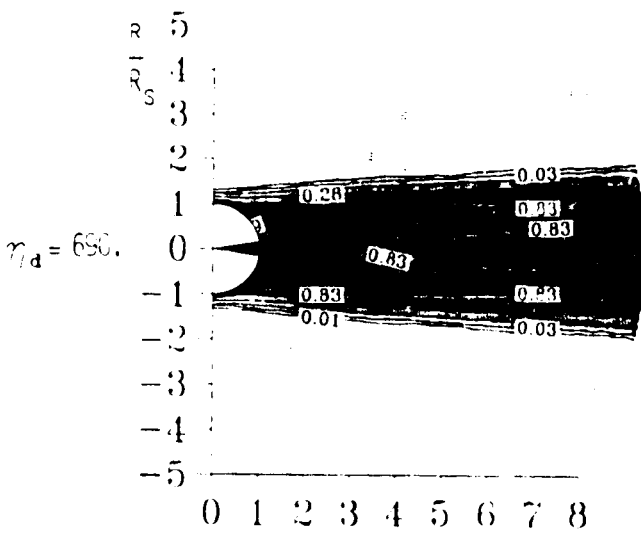
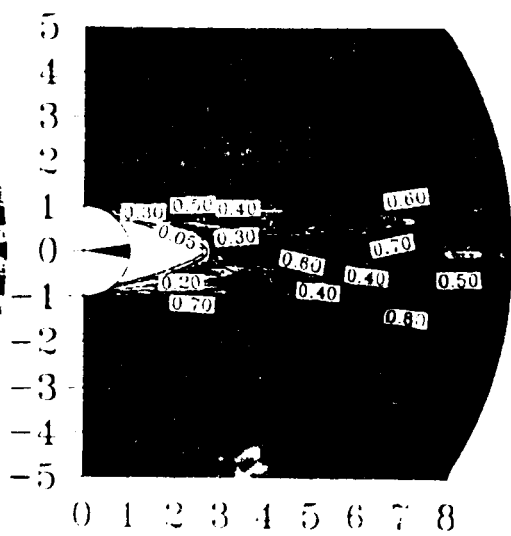
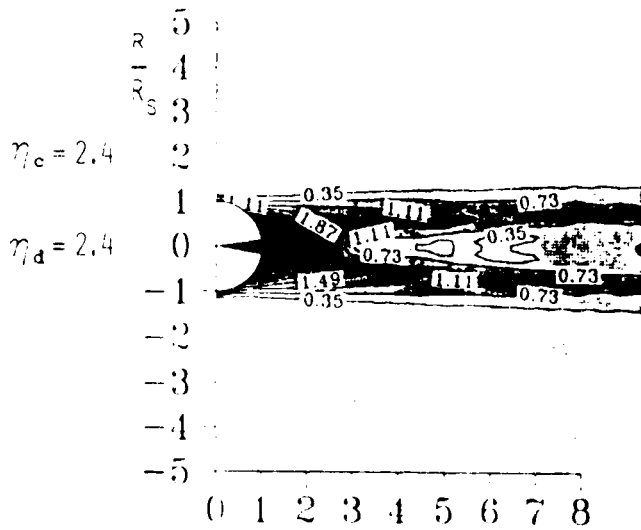
$(r, \theta)$  : polar coordinates



**FIGURE 3 :**

Numerical algorithm for the resolution of the coupled Hamilton's and Poisson's equations.

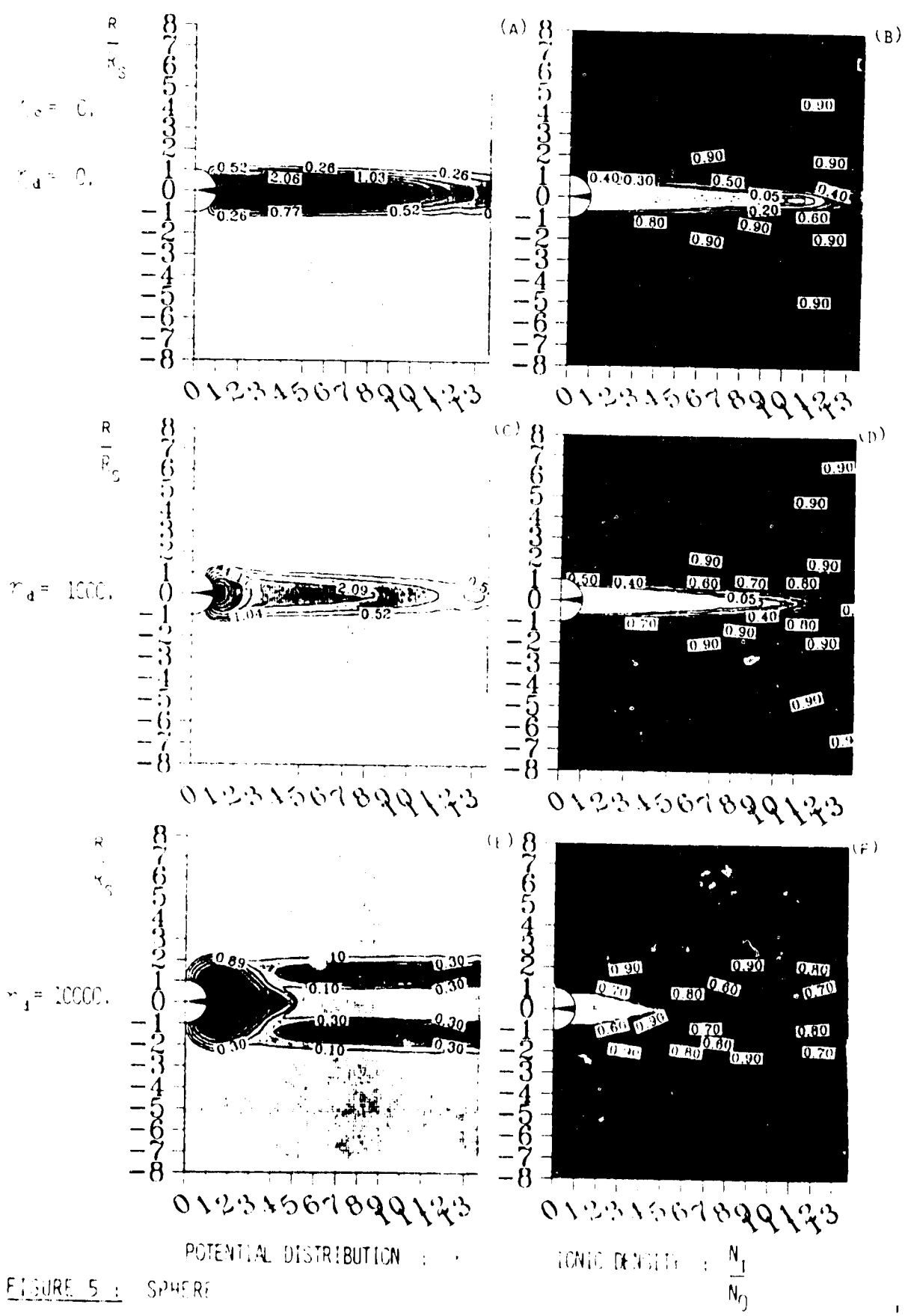




POTENTIAL DISTRIBUTION

CONTOUR PLOT

FIGURE 4 : SPHERE



POTENTIAL DISTRIBUTION : IONIC DENSITY :  $\frac{N_1}{N_0}$

FIGURE 5 : SPHERE



**TABLE 1:**

Ionospheric Parameters around 500 km high. This plasma is colder and denser than the one at geostationary orbit.

**VELOCITIES**

<b>electron or ion thermal energy :</b>	1000 °K $\approx$ 0.1 eV
<b>Electron thermal speed :</b>	$2 \cdot 10^5 \text{ m.s}^{-1}$
<b>Ion (<math>O^+</math>) thermal speed :</b>	$10^3 \text{ m.s}^{-1}$
<b>Spacecraft velocity :</b>	$8 \cdot 10^3 \text{ m.s}^{-1}$

**DENSITY**

<b>Plasma density :</b>	$10^{10} \text{ m}^{-3}$
-------------------------	--------------------------

**LENGTHS**

<b>Electron-ion mean free path :</b>	$10^4 \text{ m}$
<b>Ambient Debye length :</b>	$2 \cdot 10^{-2} \text{ m}$
<b>Ambient Electron gyroradius :</b>	$3 \cdot 10^{-2} \text{ m}$
<b>Ambient Ion (<math>O^+</math>) gyroradius:</b>	5 m

**TABLE 2 :**

Characteristics of a middle-class spacecraft and its environment in low earth orbit. The satellite radius is much greater than the Debye length, contrary to geostationary orbit conditions.

$R_{sat.}$	= 1 m
$T_e = T_i$	= .15 eV
$m_j (O^+)$	= $2.66 \times 10^{-26}$ kg
$V_{sat}$	= $8. \times 10^3$ m.s <sup>-1</sup>
$N_0$	= $1. \times 10^{10}$ m <sup>-3</sup>
$\phi_c = \phi_{float.}$	= -.36 V
$\phi_d$	= -.36, -100., -1000. V

Normalised Parameters used by the code :

$\eta_c = -\phi_c / T(eV)$	= 2.4
$\eta_d = -\phi_d / T(eV)$	= 2.4, 690., 6900.
$\zeta = R_{sat} / \lambda_{Debye}$	= 35.
$M_j = V_{sat} / V_{th.i}$	= 8.4

**TABLE 3 :**

Characteristics of a mock-up and its environment in a plasma chamber. This plasma is denser and drifts faster than the ionospheric one, around a structure much smaller than a real satellite.

$R_{sat}$	= 0.1 m
$T_e = T_i$	= 0.1 eV
$m_j (Ar^+)$	= $5.98 \times 10^{-26}$ kg
$V_{sat}$	= $15. \times 10^3$ m.s <sup>-1</sup>
$N_0$	= $1. \times 10^{11}$ m <sup>-3</sup>
$\phi_c$	= 0. V
$\phi_d$	= 0., -100., -1000. V

Normalised Parameters used by the code :

$\eta_c = -\phi_c / T(eV)$	= 0.
$\eta_d = -\phi_d / T(eV)$	= 0., 1000., 10000.
$\zeta = R_{sat} / \lambda_{Debye}$	= 13.
$M_j = V_{sat} / V_{th.i}$	= 29.